J Biol Inorg Chem (2013) 18:993–1003
DOI 10.1007/s00775-013-1048-7

ORIGINAL PAPER

Synthesis, characterization, and DNA binding of a novel ligand and its Cu(II) complex

Mei-Jin Li · Tao-Yu Lan · Zhi-Shan Lin · Changqing Yi · Guo-Nan Chen

Received: 12 June 2013 / Accepted: 4 September 2013 / Published online: 1 October 2013

Abstract A novel naphthalene-2,3-diamine-2-salicylaldehyde (NS) ligand and its mononuclear copper(II) complex (CuNS) have been synthesized and structurally characterized. The UV–vis absorption and emission spectra of NS showed obvious changes on addition of Cu^{2+} solution. The interaction of the compounds with calf thymus DNA and G-quadruplex DNA were investigated by spectroscopic methods and thermal melting assay. The nucleolytic cleavage activity of the compounds was investigated on double-stranded circular pBR322 plasmid DNA and G-quadruplex DNA by electrophoretic mobility shift assay. The results show that CuNS has a greater ability to stabilize G-quadruplex DNA over calf-thymus DNA. The cytotoxicity of the compounds toward HpeG2 cancer cells was also studied, and they showed significant potential for antineoplastic effects.

Keywords Copper(II) complex · DNA binding · Cytotoxicity · Nucleolytic cleavage

Introduction

One of the most widely applied ligands in coordination chemistry is a Schiff base, in which the special structure of the C=N bond and the oxygen atoms as the electron donor in the hydroxyl group can complex well with metal ions. Studies of a new kind of chemotherapeutic Schiff base are now attracting the attention of biochemists [1, 2]. Earlier work [3–5] reported that some drugs showed increased activity when they were administered as metal complexes rather than as organic compounds. Transition metal complexes have shown great application prospects as anticancer drugs and DNA structural probes [6–12] in recent years. DNA is the primary target molecule for most anticancer and antiviral therapies. G-quadruplex DNA is a functionally useful secondary DNA structure containing G-quartets stabilized through Hoogsteen hydrogen bonding [13–15]. G-quadruplexes have recently received great attention because they can inhibit telomere maintenance provided by telomerase activity, thus affecting the life span of the cells of a number of cancer types [16, 17]. Investigation of interactions of DNA with small molecules is important in the development of DNA molecule probes and chemotherapeutics. A number of promising small molecules have also been devised to selectively promote the formation and/or stabilization of G-quadruplex structures [18–24]. Therefore, studying the mode and the mechanism of interaction of transition metal complexes with DNA and

Electronic supplementary material The online version of this article (doi:10.1007/s00775-013-1048-7) contains supplementary material, which is available to authorized users.

M.-J. Li (✉) · T.-Y. Lan · Z.-S. Lin · G.-N. Chen
Key Laboratory of Analysis and Detection Technology for Food Safety (Ministry of Education and Fujian Province), Department of Chemistry, Fuzhou University, Fuzhou 350108, People's Republic of China
e-mail: mjli@fzu.edu.cn

M.-J. Li
Beijing Synchrotron Radiation Laboratory, Institute of High Energy Physics, The Chinese Academy of Sciences, Beijing 100039, China

C. Yi
School of Engineering, Sun Yat-Sen University, Guangzhou 510275, People's Republic of China

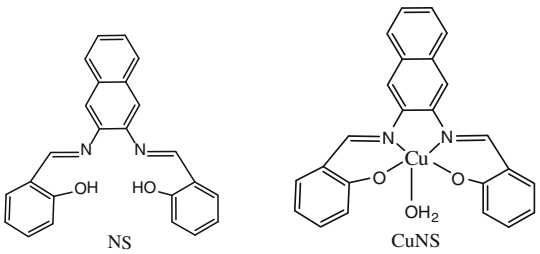

Fig. 1 Chemical structures of the Schiff base ligand (*NS*) and its copper(II) complex (*CuNS*)

exploring the application of metal complexes in antineoplastic medication, molecular biology, and bioengineering have become hot topics in recent years.

Although metal-salen and metal–salphen complexes have previously been shown to interact with duplex DNA [25–27], there are relatively few reports on the stabilization of quadruplex structures [28]. Here we report the synthesis, structure, and characterization of the novel naphthalene-2,3-diamine-2-salicylaldehyde (NS) ligand and its copper(II) complex (CuNS) (Fig. 1). The molecular probe of NS was investigated by UV–vis absorption and emission spectroscopy on addition of Cu^{2+}. The binding activities of the complex with calf thymus DNA (CT-DNA) and G-quadruplex DNA were studied by spectroscopic methods and viscosity measurements. The nucleolytic cleavage activity of the compounds was investigated by electrophoretic mobility shift assay (EMSA) experiments. The results demonstrated that combining NS with the copper(II) ion would result in stabilization of quadruplex DNA. The cytotoxicity of the compounds toward HpeG2 cancer cells was also studied, and it was found that they have significant potential for antineoplastic effects.

Materials and methods

All reagents were used as received and solvents were purified by standard methods. Naphthalene-2,3-diamine was purchased from Alfa Aesar. CT-DNA was purchased from Sigma-Aldrich (India). Ethidium bromide (EB) was purchased from Aladin Chemistry. The supercoiled pBR322 plasmid DNA and G-quadruplex DNA oligonucleotide (5′-CATGGTGGTTTGGGTTAGGGTTAGGGTTAGGGTTACCAC-3′) were obtained from Sangon (Shanghai) Biotechnology, and G-quadruplex was purified by denaturing polyacrylamide gel electrophoresis. Intramolecular G-quadruplexes was formed as follows: the G-quadruplex samples were annealed in tris(hydroxymethyl)aminomethane (Tris)–HCl–NaCl (TBS) buffer solution (5 mM Tris, 50 mM NaCl, pH 7.2) at 95 °C for 5 min, which was slowly cooled to room temperature, and was then incubated at 4 °C overnight. Other chemicals such as $Cu(CH_3COO)_2{\cdot}H_2O$ and salicylaldehyde were of analytical grade and were used without further purification. TBS buffer solution (5 mM Tris, 50 mM NaCl, pH 7.2) was used for CT-DNA binding experiments and G-quadruplex binding experiments. Tris buffer (10 mM Tris–HCl, pH 7.6, and 1 mM EDTA) was used for gel electrophoresis experiments.

Synthesis of NS

The Schiff base NS was prepared by adding salicylaldehyde (80 μL, 0.639 mmol) to a solution of 2,3-diaminonaphthalene (50 mg, 0.316 mM) in anhydrous ethanol under a nitrogen atmosphere. The mixture was heated to reflux for 4 h, and then a large amount of precipitate was formed. After the mixture had been cooled to room temperature, it was filtered, and an orange solid was obtained. The resultant orange solid was dissolved in a few drops of dichloromethane, and a small amount of *n*-hexane was added. Orange crystals of NS were obtained in about 2–3 days. Positive-ion electrospray ionization mass spectrometry (ESI-MS) (CH_2Cl_2): $m/z = 367.3$ ($[M + H]^+$). ^{1}H NMR (300 MHz, CD_3Cl, Me_4Si, δ, ppm): 12.95 (b, 2H, aromatic C–OH), 8.75 (s, 2H, –N=CH–), 7.86 (q, 2H, $J = 6.2$ Hz, $J = 2.9$ Hz, naphthalene H), 7.60 (s, 2H, naphthalene H), 7.48 (q, 2H, $J = 7.7$ Hz, $J = 1.6$ Hz naphthalene H), 7.42 (d, 2H, $J = 8.4$ Hz, benzene H), 7.40 (t, 2H, $J = 7.1$ Hz, benzene H), 7.07 (d, 2H, $J = 8.2$ Hz benzene H), 6.96 (t, 2H, $J = 7.5$ Hz, benzene H). IR (KBr disk, ν, cm^{-1}): 1,607 (C=N). 1,567, 1,499, 1,468 (ArC).

Synthesis of CuNS

$Cu(CH_3COO)_2{\cdot}H_2O$ (15.3 mg, 0.0764 mmol) was added to a solution of NS (28 mg, 0.0764 mmol) in anhydrous ethanol under a nitrogen atmosphere. The mixture was heated to reflux for 4 h, and then a brown precipitate was formed. After the mixture had been cooled to room temperature, it was filtered and washed with 95 % ethanol to give an orange solid. Recrystallization from dimethyl sulfoxide (DMSO)–acetonitrile afforded the desired CuNS as needlelike brown crystals. Positive-ion ESI-MS (CH_2Cl_2): $m/z = 428.0$ ($[M + H]^+$). Anal. Calcd for $C_{24}H_{18}N_2O_3Cu{\cdot}0.5H_2O$ (%): C, 63.30; H, 4.18; N, 6.15. Found (%): C, 63.01; H, 4.26; N, 6.39. IR (KBr disk, ν, cm^{-1}): 1,605 (C=N), 1,583, 1,524, 1,445 (ArC).

Physical measurements

^{1}H NMR spectra were recorded with a Bruker AVANCE III 300 MHz spectrometer with chemical shifts (parts per million) relative to tetramethylsilane. Positive-ion ESI-MS was performed with a Thermo Finnigan LCQ Deca XP mass spectrometer (Finnigan, USA). Elemental analyses

(C, H, N) were performed with a Vario MICRO instrument. UV–vis absorption spectra were recorded with a Lambda 750 spectrophotometer. Emission spectra were recorded with a Hitachi fluorescence F-4600 spectrophotometer (photomultiplier tube voltage 700V). Circular dichroism (CD) spectra were recorded with an AVIV model 420 spectropolarimeter. Fourier transform IR spectra were recorded as KBr pellets with a Thermo Fisher Nicolet 6700 Fourier transform IR spectrophotometer.

Single-crystal X-ray diffraction studies

The crystal structures of NS and CuNS were obtained by the single-crystal X-ray diffraction technique. The crystallographic data collection for NS and CuNS was performed on beam line 3W1A at the Beijing Synchrotron Radiation Facility with a mounted MarCCD-165 detector using synchrotron radiation ($\lambda = 0.7500$ Å) at 20 °C. Data reduction and numerical absorption correction were applied using the HKL-2000 software package [29]. The structures were solved by direct methods or the Patterson procedure, and the heavy atoms were located from E-map. The remaining non-hydrogen atoms were determined from the successive difference Fourier syntheses. All non-hydrogen atoms were refined anisotropically. The hydrogen atoms were generated geometrically with isotropic thermal parameters. Crystal parameters and details of the data collection and refinement are given in Table 1.

Table 1 Crystallographic data for naphthalene-2,3-diamine-2-salicylaldehyde (*NS*) and CuNS

	NS	CuNS
Empirical formula	$C_{24}H_{18}N_2O_2$	$C_{24}H_{18}N_2O_3Cu$
Formula weight	366.40	445.95
Space group	*P*21	*P*2(1)/*c*
a (Å)	6.1450 (12)	17.552 (3)
b (Å)	9.2040 (18)	19.896 (4)
c (Å)	16.209 (3)	5.073 (1)
α (°)	90	90
β (°)	93.57 (3)	90
γ (°)	90	90
V (Å^3)	915.0 (3)	1,771.6 (6)
Z	2	4
ρ_{calcd} (g cm^{-3})	1.330	1.672
μ (mm^{-1})	0.086	1.462
F(000)	384.0	916.0
$R_1(F_o)$[a]	0.0244 (2,615)	0.0968 (2,725)
$wR_2(F_o^2)$[b]	0.0673 (2,636)	0.2201 (2,782)
Goodness of fit	1.065	1.309

[a] $R_1 = \sum |F_o - F_c| / \sum |F_o|$

[b] $wR_2 = \left\{ \sum \left[w\left(F_o^2 - F_c^2\right)^2 \right] / \sum \left[w\left(F_o^2\right)^2 \right] \right\}^{1/2}$

Absorption and emission titrations

The NS and CuNS stock solutions were prepared in DMSO, and then they were diluted with buffer. The UV–vis absorption experiments for DNA binding were performed in 6.6 % DMSO–TBS buffer solution (pH 7.2). The absorbance of NS at 335 nm and that of CuNS at 425 nm was measured after titration with CT-DNA. The data were then fit to Eq. 1 [30] to obtain the intrinsic binding constant K_b:

$$[\mathrm{DNA}]/[\varepsilon_a - \varepsilon_f] = [\mathrm{DNA}]/[\varepsilon_b - \varepsilon_f] + 1/K_b[\varepsilon_b - \varepsilon_f] \quad (1)$$

where [DNA] is the concentration of DNA in base pairs, ε_a is the extinction coefficient observed for the absorption band at the given DNA concentration, ε_f is the extinction coefficient of the complex free in solution, and ε_b is the extinction coefficient of the complex when fully bound to DNA.

The emission experiment was performed in 6.6 % DMSO-TBS solution with various concentrations of CT-DNA (0–320 μM) or G-quadruplex DNA (0–16 μM) and a constant concentration of NS solution (4 μM) at room temperature (excitation at 400 nm).

Circular dichroism

CD was measured with an AVIV model 420 spectropolarimeter at a scanning rate of 2.5 nm s^{-1} at 25 °C, using 1 mm path quartz cuvettes. The concentration of DNA was 1×10^{-4} M. The compounds were titrated into the DNA solution stepwise, with the DNA-to-compound ratio ranging from 10:0.5 to 10:5. The working solution was incubated for 5 min after each addition. A solution of G-quadruplex (10 μM) was prepared in TBS buffer, and then solutions of NS and CuNS (0–40 μM) in DMSO were added. The CD signals of TBS were subtracted as the background.

Thermal denaturation studies

DNA thermal denaturation studies were performed by monitoring the absorption intensity of CT-DNA (50 μM) in 1.6 % DMSO–TBS buffer solution (pH 7.2) at 266 nm by varying the temperature from 30 to 95 °C in the absence and in the presence of the different compounds with a compound to CT-DNA molar ratio of 1:10. G-quadruplex thermal denaturation studies were performed by monitoring the absorption intensity of G-quadruplex (1 μM) in 5.5 % DMSO–TBS buffer solution (pH 7.2) at 295 nm by varying the temperature from 40 to 90 °C in the absence and in the presence of NS or CuNS at a molar ratio of complex to G-quadruplex of 1:1. The T_m values were determined graphically from the plots of absorbance versus temperature.

Chemical nuclease activity

The DNA cleavage studies were performed by agarose gel electrophoresis on a 15-μL sample volume containing pBR322 DNA (100 ng/μL) in 5 % dimethylformamide and 95 % Tris buffer (10 mM Tris–HCl, pH 7.6, and 1 mM EDTA). For the gel electrophoresis experiments, supercoiled pBR322 DNA was treated with different concentrations of the compounds or was treated with different concentrations of the compounds and H_2O_2 as a reducing agent. The mixtures were incubated in the dark for 30 min at 37 °C, followed by addition of a loading buffer containing 0.25 % bromophenol blue, 0.25 % xylene xyanol FF, and 60 % glycerol (3 μL) to the mixture. The samples were analyzed by 1 % agarose gel electrophoresis (Tris–borate–EDTA buffer, pH 7.6) for 3 h at 60 V. The gels were stained with EB at a concentration of 0.5 μg mL^{-1} and were visualized by UV light and photographed for analysis.

Electrophoretic mobility shift assay

EMSA was performed by maintaining the concentration of G-quadruplex (0.7 μL, 10 μM), which was heated at 95 °C for 5 min in TBS buffer (pH 7.2). After the DNA had cooled to room temperature, a 10-mL stock solution of the metal complex was added to each sample to produce the specified concentrations in a total volume of 15 mL. The reaction mixture was incubated for 12 h at room temperature. 3 mL of loading buffer (0.25 % bromophenol blue, 0.25 % xylene xyanol FF, 60 % glycerol) was added to the mixture, and it was analyzed by 20 % native polyacrylamide gel electrophoresis (the gel was prerun for 30 min). Electrophoresis proceeded for 3 h in Tris–borate EDTA running buffer. The gels were silver-stained according to a previously reported protocol [31, 32].

Cytotoxicity studies

Cytotoxicity studies were conducted on the HepG2 cell line using the 3-(4,5-dimethylthiazol-2-yl)-2,5-diphenyltetrazolium bromide (MTT) assay method [33]. The procedure was the same as in a previous report [34], except that NS and CuNS were used to treat HepG2 cells.

Results and discussion

Synthesis and characterization

NS was prepared by reaction of 2,3-diaminonaphthalene with salicylaldehyde in anhydrous ethanol solution at 78 °C for 4 h, and was recrystallized from dichloromethane–*n*-hexane. CuNS was synthesized directly from the reaction of NS with $Cu(CH_3COO)_2{\cdot}H_2O$ in anhydrous ethanol solution at 78 °C for 4 h, and was recrystallized from DMSO–acetonitrile. NS and CuNS were characterized by ESI-MS, which showed molecular ion fragments $[M + H]^+$ as the principal peak with high abundance. NS and CuNS were further characterized by IR spectroscopy. NS showed vibration bands for C=N (1,607 cm^{-1}) and ring-breathing vibrations of the aromatic rings (CC) (1,567, 1,499, and 1,368 cm^{-1}). CuNS showed vibration bands for C=N (1,605 cm^{-1}) and ring-breathing vibrations of the aromatic rings (CC) (1,584, 1,526, 1,445 cm^{-1}). NS gave a well-defined ^1H NMR spectrum, which permitted unambiguous identification and assessment of purity. A broad band corresponding to phenyl–OH was observed at 12.95 ppm, and a singlet peak was observed for the proton of –N=CH– at 8.75 ppm. CuNS give a satisfactory elemental analysis corresponding to the desired metal complex. NS and CuNS were also characterized by the single-crystal X-ray structure.

Crystal structures

Single crystals of NS suitable for X-ray diffraction were grown by vapor diffusion of *n*-hexane into a concentrated dichloromethane solution of NS. Single crystals of CuNS suitable for X-ray diffraction were grown by vapor diffusion of acetonitrile into a concentrated DMSO solution of CuNS The solid-state structures of NS and CuNS were determined by X-ray crystallography, and ORTEP drawings of NS and CuNS are depicted in Fig. 2. The crystal system of NS belongs to the *P*21 space group, and the N1–C7 and N2–C18 bond distances are 1.2902 and 1.2838 Å, respectively. The crystal system of CuNS belongs to the *P*2(1)/*c* space group, with the metal center in a 4 + 1 square-pyramidal CuN2O3 coordination geometry, the apical site being occupied by a coordinated water molecule. The donor atoms in each basal plane are two nitrogen atoms (N1, N2) and two *ortho* oxygen atoms (O1, O2). The apical site has a coordinated water molecule with a Cu1–O1W distance of 2.220 Å for CuNS compared with the equatorial Cu–O distance of 1.93–1.99 Å. Selected bond lengths and angles for NS and CuNS are listed in Table 2.

Photophysical properties

The absorption spectra of NS and CuNS in DMSO solution are shown in Fig. 3. The photophysical data for NS and CuNS are listed in Table 3. The absorption bands of NS at 272 and 338 nm correspond to intraligand transitions of the ligand. The absorption bands of CuNS at 269 and 321 nm correspond to intraligand transitions of π to π^* orbitals of the ligand, and the band at 424 nm was assigned as the

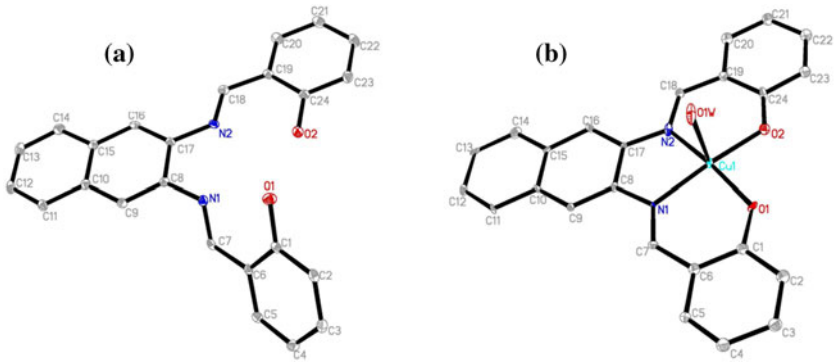

Fig. 2 ORTEP drawings of **a** NS and **b** CuNS with the atom labeling scheme showing 30 % thermal ellipsoids

Table 2 Selected bond distances (Å) and angles (°) for the NS and CuNS

NS		CuNS	
N(2)–C(18)	1.2838 (18)	Cu(1)–O(1)	1.885 (8)
N(2)–C(17)	1.4143 (18)	Cu(1)–O(2)	1.900 (8)
C(8)–N(1)	1.4256 (16)	Cu(1)–N(2)	1.918 (9)
N(1)–C(7)	1.2902 (17)	Cu(1)–N(1)	1.955 (8)
C(18)–N(2)–C(17)	123.53 (11)	Cu(1)–O(1W)	2.220 (9)
C(16)–C(17)–N(2)	124.81 (12)	O(1)–Cu(1)–O(2)	88.7 (4)
N(2)–C(17)–C(8)	115.90 (11)	O(1)–Cu(1)–N(2)	172.1 (4)
C(9)–C(8)–N(1)	120.94 (11)	O(2)–Cu(1)–N(2)	93.5 (3)
N(1)–C(8)–C(17)	118.96 (11)	O(1)–Cu(1)–N(1)	92.1 (3)
C(7)–N(1)–C(8)	117.98 (11)	O(2)–Cu(1)–N(1)	171.4 (4)
N(1)–C(7)–C(6)	121.93 (12)	N(2)–Cu(1)–N(1)	84.6 (4)
N(1)–C(7)–H(7A)	119.0	O(1)–Cu(1)–O(1W)	94.4 (4)
N(2)–C(18)–C(19)	120.66 (12)	O(2)–Cu(1)–O(1W)	97.5 (3)
N(2)–C(18)–H(18A)	119.7	N(2)–Cu(1)–O(1W)	92.9 (4)
		N(1)–Cu(1)–O(1W)	91.0 (4)
		C(1)–O(1)–Cu(1)	129.9 (7)
		Cu(1)–O(1W)–H(1WA)	109.3
		C(24)–O(2)–Cu(1)	125.9 (7)
		C(7)–N(1)–Cu(1)	123.5 (7)
		C(8)–N(1)–Cu(1)	111.6 (6)
		C(18)–N(2)–Cu(1)	126.0 (7)
		C(17)–N(2)–Cu(1)	113.0 (7)

ligand-to metal-transition of CuNS. The low-energy band around 600 nm for CuNS was assigned as the metal *d–d* transition typical of copper(II) complexes [35, 36].

On addition of Cu^{2+} (0.001–15 equiv) to the solution of NS in DMSO, the absorption band at 272 nm increased in intensity with no obvious shift, whereas the absorption band at 338 nm increased in intensity and underwent a blueshift of 17 nm. A new peak at 424 nm appeared on the addition of Cu^{2+} (Fig. 4a). The new band increased in intensity and reached saturation at a molar ratio of ligand to Cu^{2+} of 1:1. All of these changes are possibly ascribed to the coordination between the metal ion (Cu^{2+}) and the ligand (NS). The results also suggested that Cu^{2+} could easily insert itself into the hole in the ligand because of the small steric hindrance of the ligand, which was able to maximize the coordination effect. The fluorescence spectrum of NS (20 μM) in DMSO exhibited an emission band at 490 nm (Fig. 4b), which can be attributed to a very fast enol-imine to keto-amine tautomerism involving the phenomenon of excited-state intramolecular proton transfer (Fig. 5) [37]. The emission intensity decreased as Cu^{2+} was added to the solution of NS and reached saturation after the addition of 5 equiv of Cu^{2+}. This might be due to the prohibition of the excited-state intramolecular proton transfer phenomenon, and hence the fluorescence was quenched. However, the fluorescence intensity of NS was

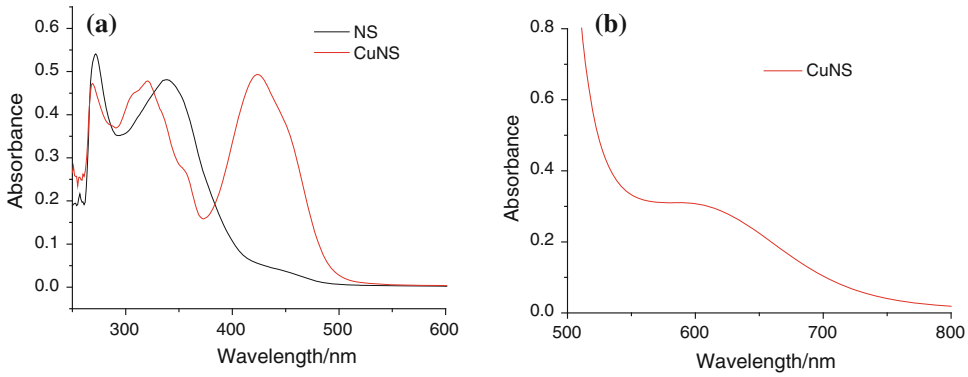

Fig. 3 **a** UV–vis spectra of NS (20 μM) and CuNS (20 μM). **b** UV–vis spectra of CuNS (1 mM)

Table 3 UV–vis data for NS and CuNS

Compound	Absorbance, λ_{max} (nm) [ε (M^{-1} cm^{-1})]
NS	272 (60,284), 338 (35,579)
CuNS	269 (49,639), 321 (47,483), 424 (49,331), 600 (307)

not completely quenched after addition of Cu^{2+} compared with CuNS, because NS could not completely complex with Cu^{2+} at room temperature.

Electrochemistry

Cyclic voltammetry of CuNS was performed with a glassy carbon electrode at a scan rate of 0.1 V s^{-1} in dimethylformamide containing *n*-Bu_4NPF_6 (0.1 M) as the supporting electrolyte; the cyclic voltammogram is shown in Fig. 6. CuNS exhibited a quasi-reversible peak attributable to Cu(II)/Cu(I) [38] at −1.46 V (ΔE_P = 100 mV) versus $Ag/AgNO_3$. The redox potential was relatively negative compared with that of a polypyridine copper(II) complex, probably owing to the strong electron-donating ability of oxygen in the hydroxyl groups after deprotonation.

Binding studies

Absorption spectroscopy studies

The DNA-binding ability of the compound was studied by an electronic absorption spectrophotometric method. On addition of CT-DNA to NS and CuNS solutions, the intensity of peak at 270 nm increased owing to the absorbance of the CT-DNA itself. The absorption bands at 339 nm (NS) and at 320 and 425 nm (CuNS) also increased in intensity, and hyperchromicity was observed, which suggested that there was an interaction between NS and CT-DNA (Fig. 7a) and between CuNS and CT-DNA (Fig. 7b). The spectral changes were ascribed to the binding of NS and CuNS to the base pairs of DNA, which made the base stacking force, hydrophobic interaction, and the van der Waals force change, and ultimately affected the conformational and structural stabilization of CT-DNA [39]. K_b of NS toward CT-DNA obtained from the regression analysis was approximately (1.8 ± 0.3) × 10^5 M^{-1}, and K_b of CuNS toward CT-DNA obtained from the regression analysis was approximately (7.1 ± 0.1) × 10^4 M^{-1}. The values were lower than those obtained for typical intercalators (e.g., EB–DNA, approximately 10^6 M^{-1}) [40], indicating that the affinity of NS and CuNS for CT-DNA was weak and the partial intercalative binding mode appeared likely.

The binding abilities of NS and CuNS with a G-quadruplex were also examined by UV–vis absorption titration experiments. An intramolecular G-quadruplex was prepared by incubating an oligonucleotide [5′-CATGGTGGTTT $(GGGTTA)_4$CCAC-3′] containing four human telomeric sequences in TBS buffer, which was heated to 95 °C for 5 min and then cooled slowly to room temperature, then kept at 4 °C overnight. On addition of the G-quadruplex to the solution of NS in TBS buffer, the absorption band at 340 nm decreased in intensity (Fig. 7c). K_b of NS toward G-quadruplex DNA obtained from the regression analysis was approximately (3.3 ± 0.1) × 10^4 M^{-1}. On addition of the G-quadruplex to the solution of CuNS in TBS buffer, the absorption band at 420 nm decreased in intensity and underwent a slight redshift, and hypochromism (22 %) of the band was observed (Fig. 7d). K_b of CuNS toward G-quadruplex DNA obtained from the regression analysis was approximately (6.5 ± 0.2) × 10^5 M^{-1}, which was larger than that of CT-DNA. The results demonstrated that CuNS showed higher affinity for G-quadruplex DNA than for nonquadruplex double-stranded DNA and the copper(II) center plays an important role in stabilizing G-quadruplex DNA.

Emission spectroscopy studies

Emission spectroscopy studies were performed through the successive additions of various concentration of DNA to the NS solution. NS was emissive at 480 nm in the absence of CT-DNA in aqueous 6.6 % DMSO–TBS solution. When the concentration of CT-DNA solution was increased, the

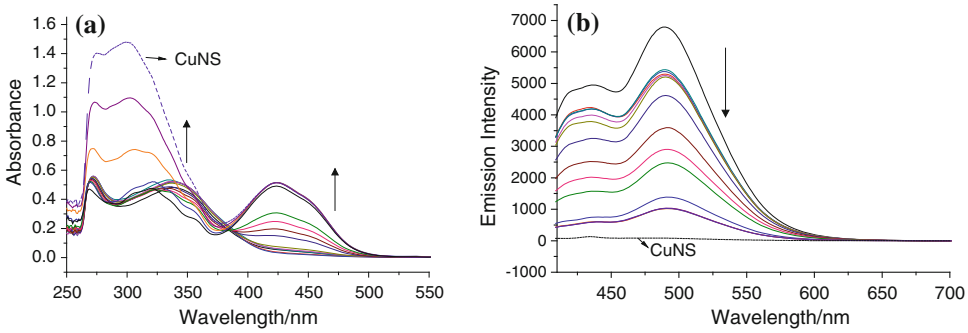

Fig. 4 **a** Absorption spectra of NS (20 μM) on the titration of Cu^{2+} (0–15 equiv) in dimethyl sulfoxide (DMSO) (*solid lines*) and absorption spectrum of CuNS (20 μM, *dashed line*) in DMSO. **b** Emission spectra of NS (20 μM) on the titration of Cu^{2+} (0–15 equiv) in DMSO (*solid lines*) and emission spectrum of CuNS (20 μM) in DMSO (*dashed line*)

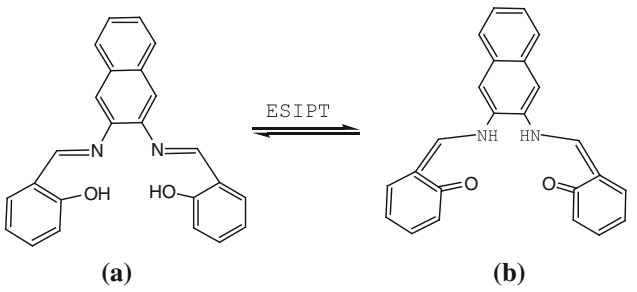

Fig. 5 Enol-imine (*A*) and keto-amine (*B*). *ESIPT* excited-state intramolecular proton transfer

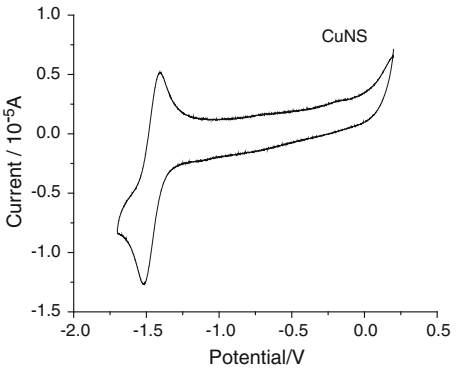

Fig. 6 Cyclic voltammogram of CuNS in dimethylformamide (0.1 M *n*-Bu_4NPF_6) with a glassy carbon working electrode. The scan rate was 0.1 Vs^{-1}

emission intensity of NS was enhanced, as shown in Fig. 8a. This is because the fluorescence of NS was weak when it was in contact with the water molecules in 6.6 % DMSO–TBS solution. After the CT-DNA had been added to the NS solution, the prevention of the interacting moieties from forming intermolecular hydrogen bonds by CT-DNA increased the hydrophobility, which contributed to the DNA-induced emission enhancement [41]. On addition of the G-quadruplex to NS, the emission intensity at 480 nm of NS decreased (Fig. 8b), and saturated at a G-quadruplex to NS concentration ratio of 2 or greater. This was because G-quadruplex was nonfluorescent, and the combination of NS with G-quadruplex DNA would cover the fluorescent part of NS. Competitive DNA binding experiments was also performed by adding different concentrations of CuNS to a solution of the EB–DNA system. However, there were no obvious emission changes (Fig. S1), because EB molecules could not be replaced completely by CuNS, which demonstrated that CuNS showed weak binding ability toward CT-DNA, in agreement with the findings from electronic absorption titrations. It seemed that combining NS with the copper(II) ion would not reinforce its binding to CT-DNA, and so the partial intercalative binding interaction between NS and CT-DNA played an important role in the high cytotoxicity of the NS ligand.

CD spectral analysis

CD spectroscopy was used to assess whether nucleic acids undergo conformational changes as a result of complex formation or changes in the environment [42, 43], because the CD spectrum of DNA is very sensitive to conformational changes. In the CD spectra, CT-DNA exhibits a positive band at approximately 280 nm due to base stacking and a negative band at approximately 245 nm due to the helicity, which is characteristic of B-DNA [44]. The addition of NS to a solution of CT-DNA induced a decrease in intensity for both the negative ellipticity band at 245 nm and the positive ellipticity band at 280 nm, as shown in Fig. 9a. Intercalation was the most probable mode of binding between NS and CT-DNA because of the planar aromatic structure of NS. After addition of CuNS, the ellipticity of the negative band at 245 nm and that of the positive band at 280 nm also decreased, as shown in Fig. 9b. Generally, covalent binding and intercalative binding could influence the tertiary structure of DNA and induce changes in the CD spectra of DNA, whereas other noncovalent binding modes such as electrostatic interaction or groove binding could not significantly perturb the CD spectra [45]. But the ability of CuNS for intercalation in DNA appeared weak.

The G-rich telomeric sequence forms intramolecular and intermolecular G-quadruplexes in monomeric, dimeric, and tetrameric structures through multiple methods [46]. CD spectroscopy provides additional support for determining the presence and to some degree the folding of G-quadruplex structures. All guanine units in the parallel-stranded G-quadruplex composed of *anti* glycosidic bond conformations have a large positive band at 295 nm and a negative band at 240 nm, whereas guanine units in the antiparallel-type G-quadruplex containing alternating *syn* and *anti* glycosyl bond conformations along each DNA strand have a characteristic positive band at 295 nm, a negative minimum at 265 nm, and a smaller positive band at 245 nm in the CD spectra [47]. Complex binding studies were conducted in the presence of a stabilizing salt by CD spectroscopy to investigate whether there was induction and conversion among various kinds of human telomeric quadruplexes. NS-induced and CuNS-induced formation of G-quadruplex structure in the absence of Na^+ was monitored using CD spectroscopy (Fig. 9c, d). The CD spectra of the human telomeric quadruplexes at room temperature exhibited a negative band centered at 239 nm and a rather broad positive signal around 273–287 nm, which showed that the quadruplex molecules exited as typical parallel G-quadruplex conformations in the presence of Na^+. On titration of NS into the G-quadruplex solution, the intensity of the CD signals corresponding to DNA was altered

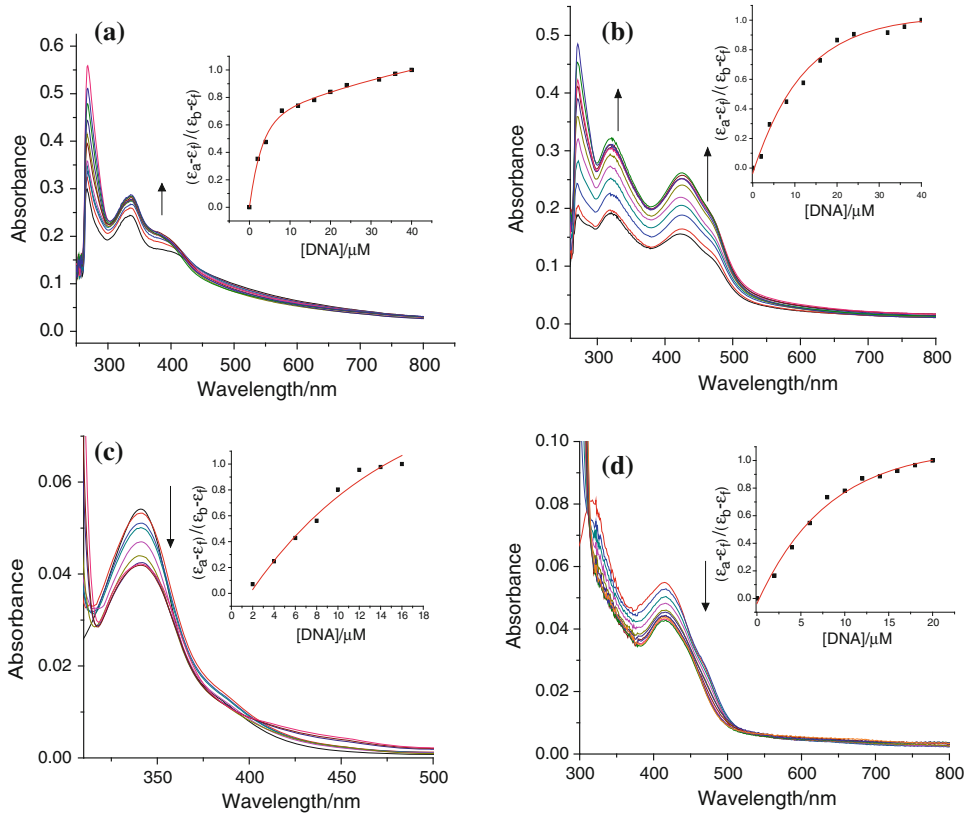

Fig. 7 **a** Absorption spectra of NS (20 μM) on the titration of calf thymus DNA (CT-DNA; 0–40 μM) in 6.6 % DMSO– tris(hydroxymethyl)aminomethane (Tris)–HCl–NaCl (TBS) solution. The *insert* shows the least-squares fits of $(\varepsilon_a - \varepsilon_f)/(\varepsilon_b - \varepsilon_f)$ versus DNA concentration for NS. **b** Absorption spectra of CuNS (20 μM) on the titration of CT-DNA (0–40 μM) in 6.6 % DMSO–TBS solution. The *insert* shows the least-squares fits of $(\varepsilon_a - \varepsilon_f)/(\varepsilon_b - \varepsilon_f)$ versus DNA concentration for CuNS. **c** Absorption spectra of NS (4 μM) on the titration of G-quadruplex (0–16 μM) in 6.6 % DMSO–TBS solution. The *insert* shows the least-squares fits of $(\varepsilon_a - \varepsilon_f)/(\varepsilon_b - \varepsilon_f)$ versus G-quadruplex concentration for NS. **d** Absorption spectra of CuNS (4 μM) on the titration of G-quadruplex (0–20 μM) in 6.6 % DMSO–TBS solution. The *insert* shows the least-squares fits of $(\varepsilon_a - \varepsilon_f)/(\varepsilon_b - \varepsilon_f)$ versus G-quadruplex concentration for CuNS

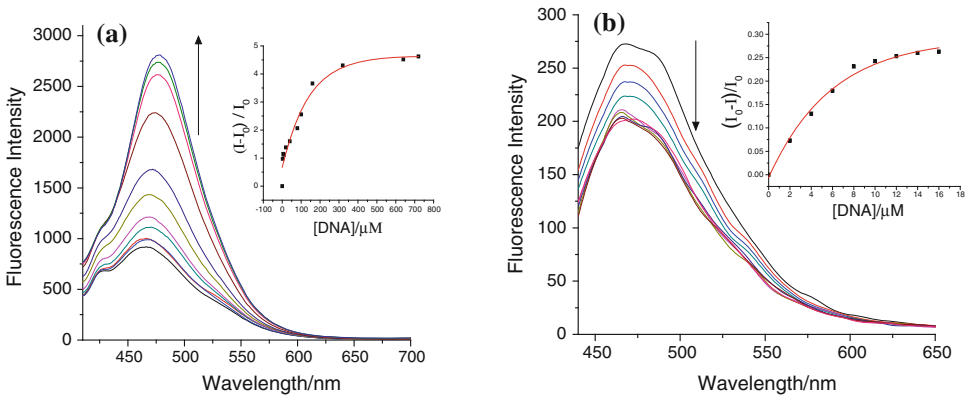

Fig. 8 **a** Emission spectra of NS (20 μM) with increasing concentration of DNA (0–320 μM) in 6.6 % DMSO–TBS solution. **b** Emission spectra of NS (4 μM) with increasing concentration of G-quadruplex (0–16 μM) in 6.6 % DMSO–TBS solution

(Fig. 9c), although no significant spectral changes were observed and the conformation of the G-quadruplex DNA did not show a clear change [48]. The negative band at 238 nm decreased in intensity, and the rather broad positive signal in the CD spectra increased in intensity and shifted to 289 nm on titration of CuNS into the G-quadruplex solution. The results suggested that CuNS could induce significant changes in the intensity of the CD signals corresponding to G-quadruplex DNA in the presence of Na^+, probably due to the structural conversion between the intramolecular and the intermolecular G-quadruplex [49–51].

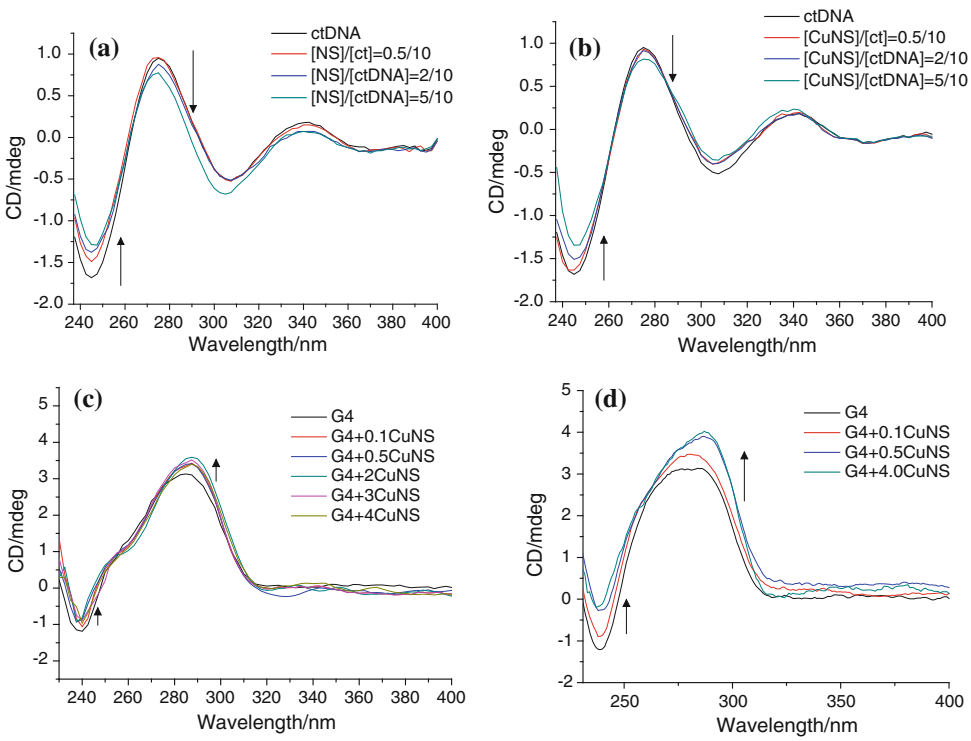

Fig. 9 Circular dichroism (*CD*) spectra of CT-DNA (200 μM) in the presence of **a** NS and **b** CuNS (0–100 μM) in TBS buffer at room temperature, and CD spectra of G-quadruplex DNA (10 μM) in the presence of **c** NS and **d** CuNS (0–40 μM) in TBS buffer at room temperature

DNA melting studies

DNA melting experiments was performed in the absence and presence of NS and CuNS at different temperatures (Fig. 10a). Such experiments could provide insight into the conformational changes and information on the strength of the interaction with DNA in the presence of the compound. The melting temperature (T_m) of CT-DNA increased by approximately 3 and 4 °C after addition of NS and CuNS, respectively. Such minor changes suggested the partial intercalative binding nature of the compound [52].

Additional evidence for G-quadruplex stabilization was provided by a thermal denaturation study. This was performed in the absence and presence of NS and CuNS at different temperatures (Fig. 10b). T_m of G-quadruplex in TBS buffer was about 68 °C, but after the G-quadruplex (10 μM) had been treated with an equimolar amount of NS, T_m increased by 6 °C. When the G-quadruplex (10 μM) was treated with an equimolar amount of CuNS, a marked increase in T_m (approximately 12 °C) was observed, suggesting CuNS showed higher affinity toward G-quadruplex DNA than toward double-stranded DNA. This result agreed with that from the UV–vis absorption and CD spectroscopy studies. It seems that combining NS with copper(II) ions reinforces its binding to G-quadruplex DNA probably because of the square-pyramidal coordination geometry [53].

DNA cleavage

The DNA cleavage ability of CuNS was studied by agarose gel electrophoresis using supercoiled pBR322 plasmid DNA as a substrate. Briefly, pBR322 DNA was mixed with different concentrations of CuNS in aqueous buffer solution (10 mM Tris–HCl, pH 7.6, and 1 mM EDTA), and the mixture was incubated at 37 °C for 30 min. With the increase of concentration of CuNS, DNA was not converted, and it did not show any cleavage activity (Fig. S1). The DNA cleavage activities of CuNS (160 μM), NS (160 μM), and $Cu(CH_3COO)_2{\cdot}H_2O$ (160 μM) using H_2O_2 or ascorbate as an activator were also observed under similar conditions (Fig. S2). However, all of them did not exhibit DNA scission activity, probably because of the low redox potentials of these complexes.

Specificity for G-quadruplex DNA by EMSA

EMSA was performed to further identify whether the compounds can facilitate the formation of G-quadruplexes or facilitate conversion between the intramolecular and intermolecular structures. In the absence of the compounds, only the band corresponding to the monomer was observed in the EMSAs, in accordance with the previous gel-shift data [54]. When increasing amounts of NS were added to G-quadruplex, no new bands formed, as shown in Fig. 11. Increasing amounts of CuNS added to G-quadruplex

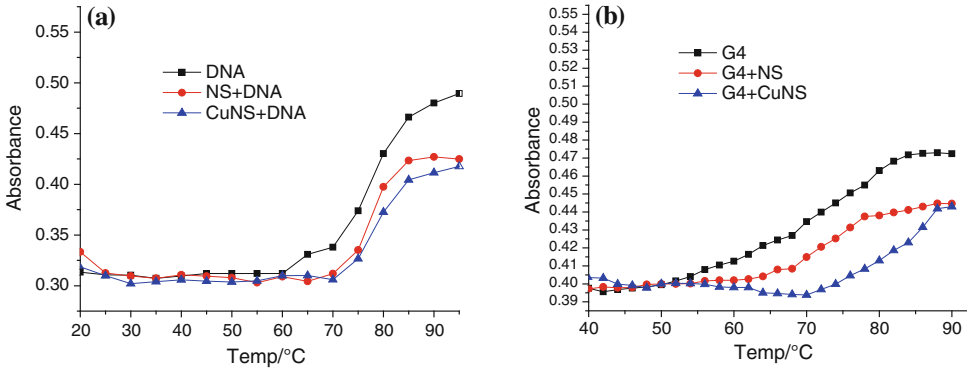

Fig. 10 **a** Thermal denaturation graphs of CT-DNA (50 μM) in the absence and presence of NS (5 μM) and CuNS (5 μM). **b** Thermal denaturation graphs of G-quadruplex DNA (10 μM) in the absence and presence of NS and CuNS (10 μM). *G4* G-quadruplex

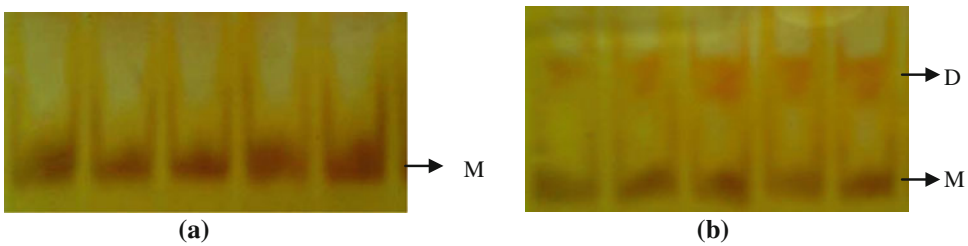

Fig. 11 Effects of NS (**a**) and CuNS (**b**) on the assembly of G-quadruplexes illustrated by polyacrylamide gel electrophoresis in TBS (pH 7.2). Major bands were identified as the monomer (*M*) and the dimer (*D*)

resulted in the progressive appearance of new bands with reduced mobility corresponding to the dimeric forms. The result showed that CuNS could efficiently promote different intermolecular quadruplex formation at high Na^+ concentration, and had a stronger quadruplex affinity than NS, showing that the copper(II) center played an important role. This observation was in good agreement with the results from CD spectroscopy, absorption spectroscopy, and melting studies in a solution of Na^+ ions.

Study of cytotoxicity by MTT assay

MTT assay was performed to check the antineoplastic effect of NS and CuNS. Their effects on cellular viability are shown in Fig. 12. Treatment of HepG2 cells with a series of dilutions (0.1, 0.5, 5, 10, and 20 μM) of NS and CuNS resulted in a decrease in cell viability. NS decreased cell viability by 47 % in 24 h at the highest dose (20 μM), whereas CuNS decreased cell viability by 83 % in 24 h at the highest dose (20 μM). The cytotoxicity as assessed by the 50% inhibitory concentration (IC_{50}) was 22.1 and 13.9 μM for NS and CuNS, respectively. Cisplatin exhibited an IC_{50} value of 28.8 μM in the control experiments. NS and CuNS exhibited IC_{50} values that are more or less equal to that of cisplatin for the same cell line, which indicates that they are promising drugs for treatment of cancer. The cytotoxicity of NS is probably due to the high affinity toward CT-DNA or complexation with the metal ion in the cell. The results revealed that the compounds, especially CuNS, exhibited severe cytotoxicity toward HepG2 cells, indicating that synergy between the metal and the ligand results in a

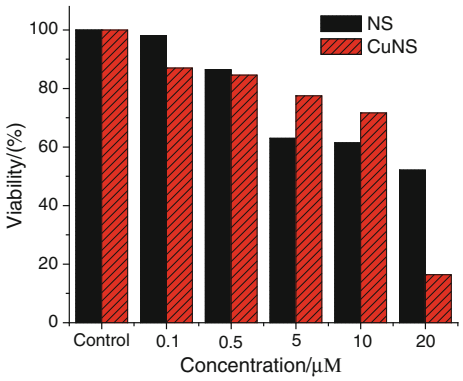

Fig. 12 The viability of HeLa cells on treatment with NS and CuNS for 24 h

significant enhancement of cell death. Although the exact mechanism for the cytotoxicity is still unclear except for cisplatin, the prominent cytotoxicity of the complex is probably related to the strong DNA binding involving hydrophobic interaction forces [55] or the dissociation of the complexes in the cell, resulting in intracellular accumulation of high amounts of copper and the chelation with biological components such as proteins from the nucleus [56].

Conclusions

A novel NS ligand and its copper(II) complex (CuNS) have been synthesized and characterized. The DNA binding properties of NS and CuNS were examined by spectroscopic methods and viscosity measurements. The larger

binding constant demonstrated that CuNS showed much higher affinity toward G-quadruplex DNA than toward CT-DNA, probably owing to its square-pyramidal coordination geometry. CD studies revealed that CuNS is a good G-quadruplex stabilizer and could keep G-quadruplexes parallel in the presence of Na^+ ions. EMSA further demonstrated that CuNS can promote conversion of G-quadruplex to the dimeric form. MTT assay showed that NS and especially CuNS are cytotoxic to the HepG2 cell line. All these findings suggest that the copper(II) center played a very important role in stabilizing G-quadruplex DNA and enhancing the cytotoxicity.

Acknowledgments This work was supported by the National Scientific Foundation of China (no. 21171038) and the Program for Changjiang Scholars and Innovative Research Team in University (no. IRT1116).

References

1. Choi YK, Chjo KH, Park SM, Doddapaneni N (1995) J Electrochem Soc 142:4107–4112
2. Bernardo K, Leppard S, Robert A, Commenges G, Dahan F, Meunier B (1996) Inorg Chem 35:387–396
3. Anitha C, Sheela CD, Tharmaraj P, Sumathi S (2012) Spectrochim Acta Part A Mol Biomol Spectrosc 98:35–42
4. Raman N, Kulandaisamy A, Jeyasubramanian K (2001) Synth React Inorg Met Org Chem 31:1249–1270
5. Tantaru G, Popescu MC, Bild V, Poiata A (2012) Appl Organomet Chem 26:356–361
6. Dardlier PJ, Holmlin RE, Barton JK (1997) Science 274:1465–1468
7. Barton JK (1986) Science 223:727–733
8. Hall DB, Holmlin RE, Barton JK (1996) Nature 382:731–735
9. Yang G, Wu JZ, Wang L, Ji LN, Tian X (1997) J Inorg Biochem 66:141–144
10. Zhang QL, Liu JG, Chao H, Xue GQ, Ji LN (2001) J Inorg Biochem 83:49–55
11. Liu JG, Ye BH, Zhang QL, Zou XH, Zhen QX, Tian X, Ji LN (2000) Biol Inorg Chem 5:119–128
12. Lo LTL, Chu WK, Tam CY, Yiu SM, Ko CC, Chiu SK (2011) Organometallics 30:5873–5881
13. Davis JT (2004) Angew Chem 116:684–716
14. Huppert JL (2008) Chem Soc Rev 37:1375–1384
15. Wang, Li Y, Tan JH, Ji LN, Mao ZW (2011) Dalton Trans 40:564–566
16. Monchaud D, Teulade-Fichou MP (2008) Org Biomol Chem 6:627–636
17. Burge S, Parkinson GN, Hazel P, Todd AK, Neidle S (2006) Nucleic Acids Res 34:5402–5415
18. Read MA, Harrison RJ, Romagnoli B, Tanious FA, Gowan SH, Reszka AP, Wilson WD, Kelland LR, Neidle S (2001) Proc Natl Acad Sci USA 98:4844–4849
19. Dixon IM, Lopez F, Esteve JP, Tejera AM, Blasco MA, Pratviel G, Meunier B (2005) ChemBioChem 6:123–132
20. Koeppel F, Riou JF, Laoui A, Mailliet P, Arimondo PB, Labit D, Petitgenet O, Helene C, Mergny JL (2001) Nucleic Acids Res 29:1087–1096
21. Clark GR, Pytel PD, Squire CJ, Neidle S (2003) J Am Chem Soc 125:4066–4067
22. Tuntiwechapikul W, Jeong TL, Salazar M (2001) J Am Chem Soc 123:5606–5607
23. Kim MY, Vankayalapati H, Shinya K, Wierzba K, Hurley LH (2002) J Am Chem Soc 124:2098–2099
24. Rajput C, Rutkaite R, Swanson L, Haq I, Thomas JA (2006) Chem Eur J 12:4611–4619
25. Mandal SS, Varshney U, Bhattacharya S (1997) Bioconjug Chem 8:798–812
26. Routier S, Cotelle N, Catteau JP, Bernier J L, Waring MJ, Riou J F, Bailly C (1996) Bioorg Med Chem 4:1185–1196
27. Muller JG, Kayser LA, Paikoff SJ, Duarte V, Tang N, Perez RJ, Rokita SE, Burrows CJ (1999) Coord Chem Rev 185:761–774
28. Reed JE, Arnal AA, Neidle S, Vilar R (2006) J Am Chem Soc 128:5992–5993
29. Otwinowski Z, Minor W (1997) Methods Enzymol 276:307–326
30. Wolfe A, Shimer GH, Meehan T (1987) Biochemistry 26:6392–6396
31. Zhou JL, Lu YJ, Ou TM, Zhou JM, Huang ZS, Zhu XF, Du CJ, Bu XZ, Ma L, Gu LQ (2005) J Med Chem 48:7315–7321
32. Sun D, Zhang R, Yuan F, Liu D, Zhou Y, Liu J (2012) Dalton Trans 41:1734–1741
33. Blagosklonny MV, EI-diery WS (1996) Int J Cancer 67:386–392
34. Li MJ, Liu X, Nie MJ, Wu ZZ, Yi CQ, Chen GN, Yam VWW (2012) Organometallics 31:4459–4466
35. Barve A, Kumbhar A, Bhat M, Joshi B, Butcher R, Sonawane U, Joshi R (2009) Inorg Chem 48:9120–9132
36. Rajendiran V, Karthik R, Palaniandavar M, Stoeckli–Evans H, Periasamay VS, Akbarsha MA, Srinag BS, Krishnamurthy H (2007) Inorg Chem 46:8208–8221
37. Bhalla V, Tejpal R, Kumar M (2011) Tetrahedron 67:1266–1271
38. Jezù owska-Bojczuk M, Les′niak W, Bal W, Kozłowski H, Gatner K, Jezierski A, Sobczak J, Mangani S, Meyer-Klaucke W (2001) Chem Res Toxicol 14:1353–1362
39. Baldini M, Belicchi-Ferrari M, Bisceglie F, Dall'Aglio PP, Pelosi G, Pinelli S, Tarasconi P (2004) Inorg Chem 43:7170–7179
40. Le Pecq JB, Paoletti CJ (1967) Mol Biol 27:87–106
41. Raja DS, Bhuvanesh NSP, Natarajan K (2011) Inorg Chem 50:12852–12866
42. Mahadevan S, Palaniandavar M (1998) Inorg Chem 37:693–700
43. Rajendiran V, Murali M, Suresh E, Palaniandavar M, Periasamy VS, Akbarsha MA (2008) Dalton Trans 16:2157–2170
44. Johnson WC (1994) In: Nakanishi K, Berova N, Woody RW (eds) Circular dichroism: principles and applications. VCH, New York, pp 523–540
45. Messori L, Orioli P, Tempi C, Marcon G (2001) Biochem Biophys Res Commun 281:352–360
46. Peti W, Meiler J, Br_schweiler R, Griesinger C (2002) J Am Chem Soc 124:5822–5833
47. Miyoshi D, Nakao A, Sugimoto N (2003) Nucleic Acids Res 31:1156–1163
48. Jain AK, Paul A, Maji B, Muniyappa K, Bhattacharya S (2012) J Med Chem 55:2981–2993
49. Xue Y, Kan Z, Wang Q, Yao Y, Liu J, Hao Y, Tan Z (2007) J Am Chem Soc 129:11185–11191
50. Lin CT, Tseng TY, Wang ZF, Chang TC (2011) J Phys Chem B 115:2360–2370
51. Liu D, Liu Y, Wang C, Shi S, Sun D, Gao F, Zhang Q, Liu J (2012) ChemPlusChem 77:551–562
52. Lahiri D, Bhowmick T, Pathak B, Shameema O, Patra AK, Ramakumar S, Chakravarty AR (2009) Inorg Chem 48:339–349
53. Bertrand H, Monchaud D, De Cian A, Guillot R, Mergny JL, Teulade-Fichou MP (2007) Org Biomol Chem 5:2555–2559
54. Han H, Langley DR, Rangan A, Hurley LH (2001) J Am Chem Soc 123:8902–8913
55. Bhat SS, Kumbhar AA, Heptullah H, Khan AA, Gobre VV, Gejji SP, Puranik VG (2011) Inorg Chem 50:545–558
56. Tardito S, Bassanetti I, Bignardi C, Elviri L, Tegoni M, Mucchino C, Bussolati O, Franchi-Gazzola R, Marchio L (2011) 133:6235–6242